MODELING OF THE EXOCYTOTIC PROCESS BY CHEMICAL KINETIC FORMALISM

Aviv Mezer[1], Esther Nachliel[1], Menachem Gutman[1] and Uri Ashery[2].

[1] The Laser Laboratory for Fast Reactions in Biology, *Department of Biochemistry. The George S Wise Faculty of Life Sciences Tel Aviv University, Tel Aviv, Israel,*
[2]*Department of Neurobiochemistry, The George S Wise Faculty of Life Sciences Tel Aviv University, Tel Aviv, Israel,*

INTRODUCTION

Exocytosis of a single vesicle is thought to be mediated by the sequence of interactions between cytosolic, vesicular and plasma membrane proteins. In the last decade, the functions of specific proteins in this process have been intensively studied. However, the exact function of most of the proteins is still not completely understood and the sequence of events has to be elucidated. In the present study we present a mathematical model that links up the partial reactions between the participating proteins into a comprehensive mechanism.

The exocytotic process, as measured by membrane capacitance measurements, can be described fitted as a sum of three exponential reactions, each representing the response of a 'pool' of vesicles to the Ca^{++} pulse. The Rapidly Releasable Pool (RRP) fuses rapidly with the cell membrane. The Slowly Releasable Pool (SRP) fuses more slowly with the cell membrane and, in parallel, matures to the RRP state. The third vesicle population is the Unprimed Pool (UPP). We shall refer to this model as a macroscopic one, as the transition between the pools is given in time constant and not by defined chemical formalism based on concentration and rate constants [1].

In our study we substitute the macroscopic description with a set of well-defined chemical (first and second order) rate reactions that, when propagated in time, reconstruct the fusion dynamics with all their fine details. Moreover, the model can also give an indication for the dynamic changes of different intermediate complexes during the exocytosis. The strength of the present model is that we can easily implement another intermediate step according to newly available data about concentration of a specific protein or information about binding kinetics.

METHODS

The mathematical model is based on a sequence of reactions that were derived by intensive study of the interactions among the various proteins involved in the exocytotic process. The reaction steps were written as a linear sequence of chemical equilibria, where the product of one step is the reactant of the next one. The equilibrium was converted into a set of differential rate equations that complies with the detailed balance principle to maintain the law of conservation of matter. The Ca^{++} was the only reactant whose concentration was kept constant even though it was taken up during the progression of the reaction, in accordance with the large intracellular reservoir of Ca^{++} ions.

The general form of the differential rate equations for the various intermediates is given by equation 1.

Eq. 1 $$\frac{\Delta C_i}{\Delta t} = -\sum_{ij} k_{ij} C_i C_j + \sum_{rs} k_{rs} C_r C_s$$

In this equation C_i and C_j are two intermediates that react one with the other with the rate constants $k_{ij.}$ C_s and C_r which are the products of the reaction and k_{rs} is the rate constant of the backward reaction.

Precise derivation of the equilibrium equations leads to a set of 16 coupled, non-linear ordinary differential equations that were propagated numerically using the ODE23S routine of Matlab 6.5R13. For the solvation of the ordinary differential equations, the program was fed with the initial concentrations of the reactants and the rate constants of the various reaction steps. The equations were propagated in time and the concentrations of the intermediates and the final product were saved as vectors. The conversion of the vectors from concentration units into the number of vesicles yielded a reconstructed signal and the adjustable parameters were modulated to match the experimental one.

The concentrations of the various reactants were either taken from the published data or derived by the search through the parameters' space. The equilibrium constant and the rate constants whose values were

already measured were taken as published, and allowed to vary as adjustable parameters within a narrow range factor of 2.

Estimation of the rate constants of the reactions

In order to estimate the rate constants of the reactions, we first used the Debye-Smoluchowski equation to calculate the maximal rate of encounter (k_{max}), where the diffusion coefficients of soluble proteins have been approximated by the Einstein Stokes equation. The diffusion coefficient of proteins on membrane was taken as 10^{-10} cm^2s^{-1}. When a single vesicle carries more than one copy of a given protein, the system loses its homogeneity; the density of the protein on the vesicle is higher than its average distribution in the whole reaction space. Consequently, the probability of a fruitful encounter of a ligand with any of the binding sites increases with the number of the sites on the vesicle's surface. Therefore, the rate constant of the encounter is a function of the density of identical binding sites carried on one vesicle, as given by Berg and Purcell [2] and given in equation 2

Eq2. $$\frac{k_{(N)}}{k_{\max}} = \frac{N \cdot r}{N \cdot r + \pi \cdot R}$$

In this equation k_{max} corresponds with the diffusion-controlled rate constant under the ideal conditions that the reactive sites cover the whole surface of the vesicular surface. This value is calculated by the Debye-Smoluchowski equation [3]. The $k_{(N)}$ is the rate constant pertinent to N identical sites evenly distributed over the surface of the vesicle. The values r and R are the radii of the site and the vesicle, respectively.

Quantitation of the concentrations and rate constants

To convert the reaction steps into a set of differential rate equations, we assigned a concentration for each reactant and defined each equilibrium with rate constants for the forward and backward directions. The parameters that had already been published were taken as a first estimation and were allowed to vary within a very narrow range from the published values. All other parameters were allowed to vary over a wide range, with an upper limit set by the estimation based on the Debye-Smoluchowski and the Berg- Purcell equations. In order to account for the discreteness of the process, the formulation of the mathematical model was carried out while expressing the number of vesicles by molar concentration. The vesicles' concentration was based on the number of morphologically docked vesicles (~1000), estimated to be in close proximity to the plasma membrane (~200-300 nm) [4, 5]. The estimated volume of the reaction space was taken as V=1.6 10^{-13} L) and corresponds to a vesicle concentration of 10 nM.

RESULTS AND DISCUSSION

The sequence of events leading to the fusion of the vesicle with the cell-membrane, The reaction rate constants and initial concentrations, are presented in scheme I

Scheme I:

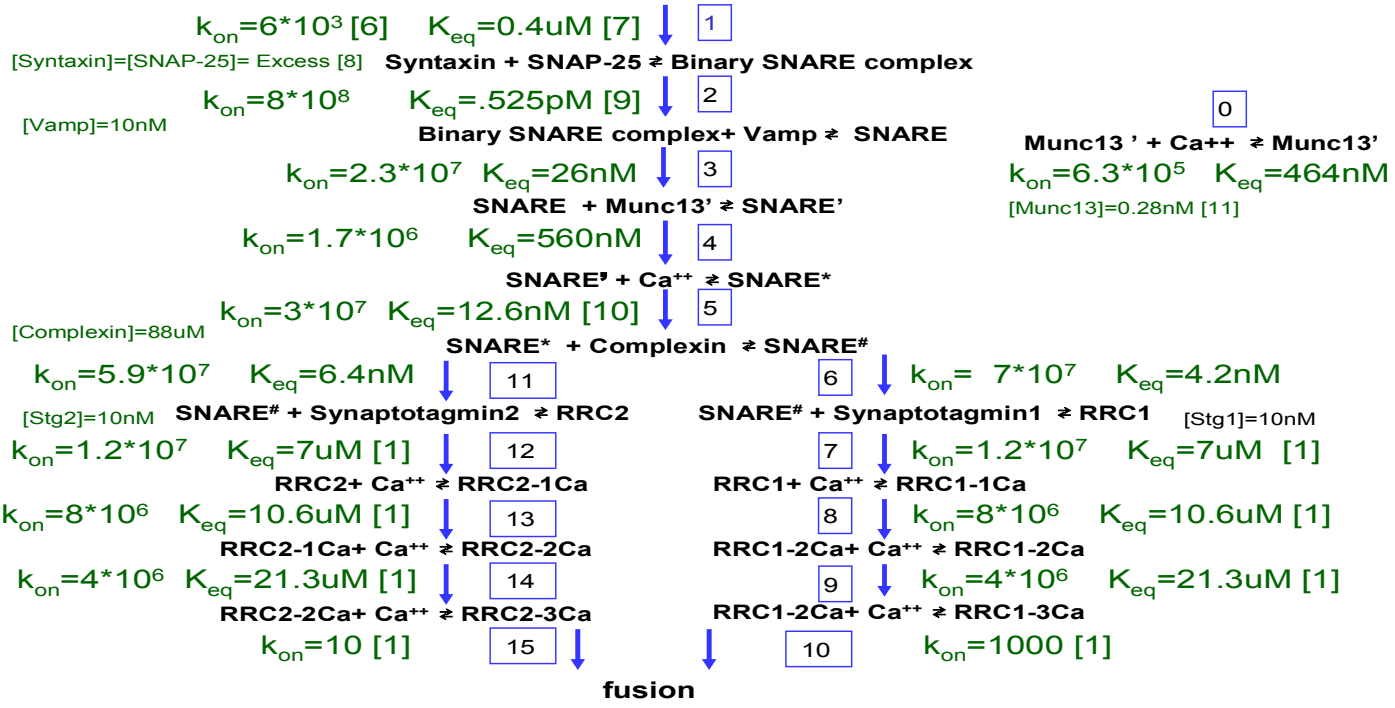

The reaction steps listed were converted into a set of coupled differential rate equations and subjected to numeric integration. The final function, corresponding with the fusion process, was multiplied by the capacitance of a single vesicle (1.25 fF) to quantitatively reconstruct the experimental signal [12].
It must be stressed that this model is a minimal one in which the sequence of reactions ignores, for example, the non-productive *cys*-SNARE complex or the reactions associated with the binding of munc18 to syntaxin. Nevertheless, the steps given in the model are those necessary and sufficient to reproduce the major macroscopic characteristics of the exocytotic process.

Reconstruction of experimental signals

Reconstruction of a Ca^{++}-triggered vesicular fusion: The reconstruction of the signals was optimized to follow the basic experimental protocol of the Ca^{++}-triggered vesicular fusion in the chromaffin cell, which consists of three steps. First, the cells are in equilibrium with low [Ca^{++}] (resting conditions). Then the intracellular Ca^{++} is increased to ~300 nM for 2 min (pre-pulse) and finally the cells are challenged by a short Ca^{++} pulse of 10-30 μM for a period of few seconds.
The simulation program reconstructed the very same protocol. At first the differential rate equations were propagated in time for 10 min, where the Ca^{++} concentration was set as 50 nM to simulate resting conditions. The various intermediates were allowed to accumulate for ten minutes. The final concentrations of the intermediates were used for the second phase of the calculations. Ca^{++} concentration was set to 280 nM to simulate the pre-pulse equilibrium for 120 seconds. The pre-pulse final intermediates values were used as the initial concentrations for the stimulation phase, where the Ca^{++} was set to be 30 μM for 5 seconds. The progression of the reaction was expressed as an integer corresponding with the number of vesicles that were fused with the cell membrane.
The incremental capacitance and reconstructed curve corresponding with the fusion step are presented in Figure 1, frame A. The main frame depicts the signal as measured over 5 seconds, while in the inset we present the expansion of the first two second of the reaction time. The accuracy of the reconstruction is very high, almost within the width of the experimental noise. The reconstruction accurately describes all the components of secretion. It starts with a very short (few milliseconds) lag phase followed by a fast initial burst, and gradually slows down to the rate of the sustained release. When subjected to macroscopic analysis (three exponent analysis [1]), the reconstructed signal yields the same size for the RRP and SRP as well as the time constants.
Synaptotagmin 1 knockout: An equivalent experiment for synaptotagmin 1 (Stg1) knockout cells resulted in a smaller and slower release. The simulation of this experiment ([synaptotagmin 1] = o) reproduces the dynamics with high accuracy (Figure 1A).
Calcium-dependent priming: Elevation of the pre-pulse calcium concentration has been shown to modulate the size of the exocytotic burst in chromaffin cells, a phenomenon known as calcium-dependent priming, and might be involved in short term plasticity processes. Figure 1B depicts the experimental observation (inset) and the outcome of the model reconstruction (main frame). Figure1B depicts the dependence of the fast release phase of the fusion on the pre-pulse Ca^{++} concentration. The experimental curve is the summation of many measurements that were carried out at varying pre-pulse Ca^{++} concentrations. The reconstructed curve is an accurate replication of the observed dependence.

Reconstruction of complex experimental protocols

The effect of over-expression of munc13: Overexpression of munc13-1 in chromaffin cells led to a 3-to 4-fold increase of exocytosis response to stimulation (inset to Figure 2A). Increasing the munc13 concentration in the mathematical model accurately reproduces the

experimental observation: a 10-fold increase of the munc13-1 replicated the amplification of the signal, matching the experimental observation.

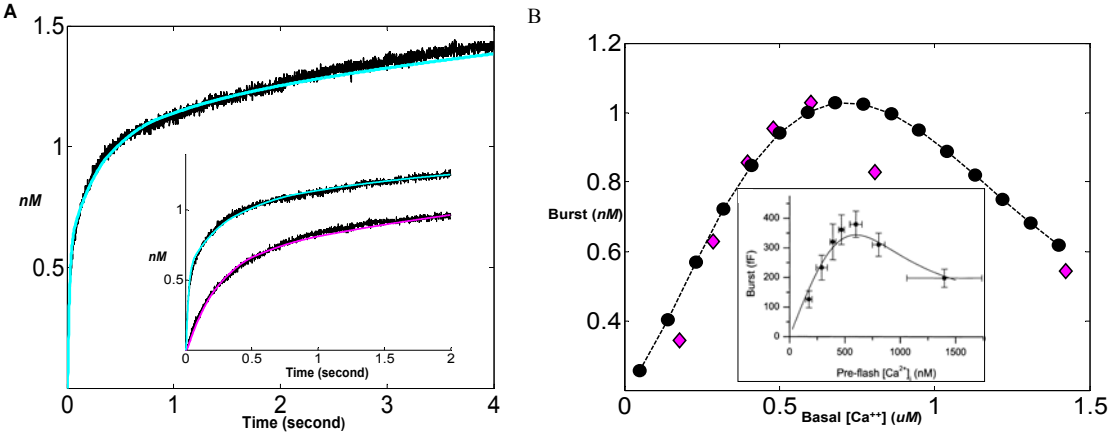

Figure 1: Frame A Reconstruction of the secretion dynamics as measured for WT cells (top curve) and for a SytIKO chromaffin cells (bottom curve.) The main frame presents the signals and their simulation over 4 second while the inset expands the first two seconds. The ordinates are quantitated in molar units. The experimental data, presented in the inset, were taken from Votes [13]]. Frame B depicts the dependence of the amplitude as measured one second after the triggering on the pre-pulse Ca^{++} concentration. The inset presents the experimental results of Voet et al [14]. The main frame depicts the prediction of the model (◊) and the experimental results (♦).

Reconstruction of multi-step experimental protocols: When chromaffin cells are repeatedly stimulated, prior to the triggering Ca^{++} pulse by a train of short depolarization pulses, there is a gradual depletion of the RRP, while the slower processes are hardly affected (see inset to Figure 2B). The simulation of the same protocol, where the depolarizations are mimicked by a 100 ms 8 μM Ca^{++} pulse, reproduced the same feature as the measurements: a gradual depletion of the fast release phase, while the other components remained practically constant.

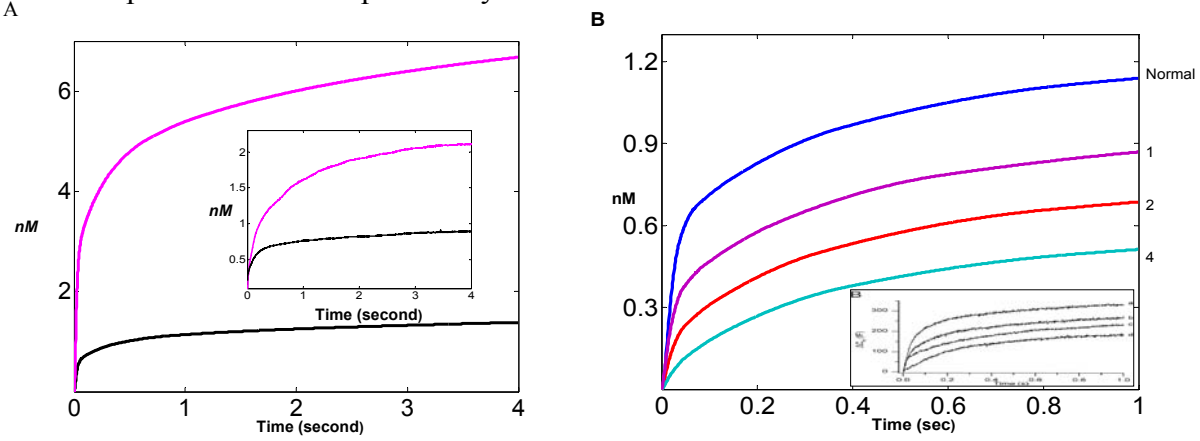

Figure 2: Reconstruction of complex experimental protocols.
Frame A: The effect of the over-expression of the munc13-1 on the release dynamics following a single Ca^{++} pulse. Mainframe depicts the release dynamics as calculated for normal munc13-1 content (0.28 nM) (Bottom) and for 10-fold increment (Top). Inset depicts the experimental observation of Ashery et at [11]). Frame B: Depicts the effect of train (1,2,4) of successive short pre-pulses, delivered before the main trigger event, on the release dynamics. Main frame reconstruction dynamics, inset experimental data [7].

The dynamics of the intermediates during the fusion process

One of the advantages of the mathematical model is that, during the reconstruction of the fusion dynamics, it generates the corresponding dynamics of all intermediates of the process. Figure 3A describe the calcium pulse effect on the intermediates. In these figures, the ordinates denote the number of vesicles that had matured to a given stage in the process.

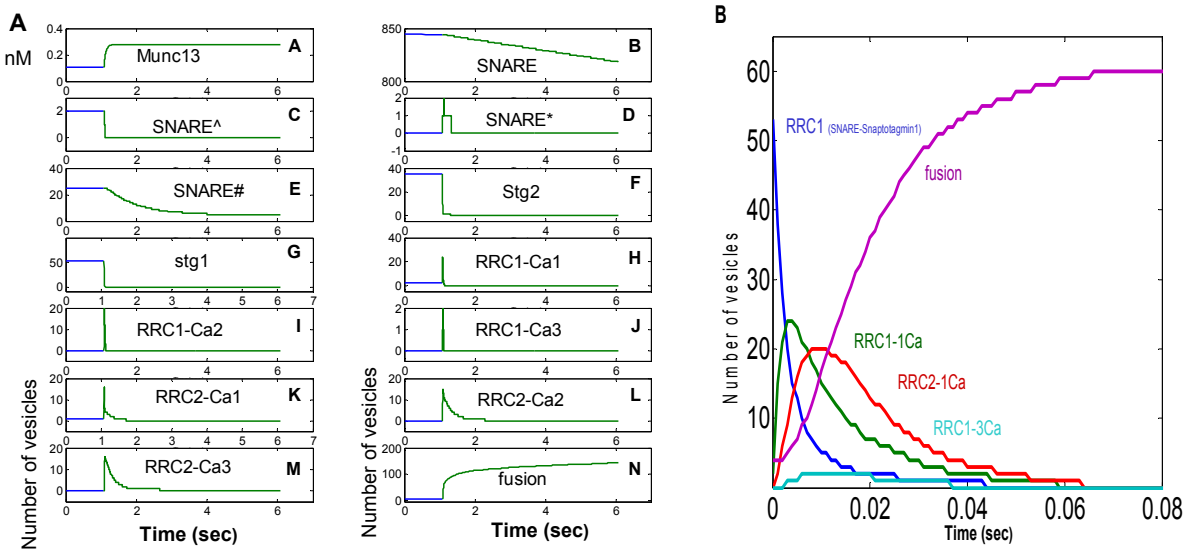

<u>Figure 3</u>: Frame A: Detailed dynamics of the individual intermediates during the fusion reaction. For clarification, the presentation is starts 1 second before the Ca^{++} pulse (green). Each frame depicts the dynamics of one intermediate, as marked in the frames. The Y-axis denotes the number of vesicles that had evolved to the pertinent state. Munc13 is given in molar units. Frame B: Superposition of the dynamics of RRC1, RRC-1Ca, RRC-2Ca· RRC-3Ca and the fusion product. All states are given as the number of vesicles and the plot describes the first 0.08 second of the reaction. Please note the time lag in the formation of the fusion product.

This analysis enables us to study the contribution of each intermediate to the different phases of the fusion. The fast kinetics, which are macroscopically defined as RRP, are related to the depletion of the "Stg1" intermediate (see Figure 3A frame G), while the SRP phase is related to the delayed release of the synaptotagmin 2 -Ca^{++} complexes that are slowly fusing with the membrane (Figure 3, frames F, K-M). The sustained phase (UPP) is contributed by upstream reactions that cause a steady consumption of the SNARE population (frames B- E).

Figure 3B presents a detailed analysis of the most initial phase of the fusion, which depicts a clear lag phase in the fusion process. The delayed fusion is accurately reconstructed (not show) by the model. The model associates the lag phase with the accumulation of the synaptotagmin 1- Ca^{++} complexes (RRC1-1Ca RRC1-2Ca RRC1-3Ca) of the synaptotagmin 1 path.

<u>CONCLUDING REMARKS</u>

In the present study we linked up the existing information into a sequence of events that are expressed by an ordinary, differential equation. The integration of the equations over time reconstructed complex experimental protocols and replicated the outcome of genetic modification of the cells. This treatment appears to bear a high predictive power and identified the protein complexes that are associated with the 'vesicular pools' as used in the multi-exponent dynamics description of the exocytotic process.

The reaction steps incorporated in the mathematical model are necessary and sufficient to reconstruct the exocytotic reaction, although it can be further expanded to account for future observations and more refined experimental observations. Most of the rate constants were found to be slower than the estimated diffusion controlled values. In these cases, we assume that the reaction pathway can incorporate more than a single step event. The hidden steps can either be a conformational change of the protein, a reaction of the indicated complex with other (still unidentified) protein(s), or even olygomerization of the complex/protein. Nevertheless, these equations can be used as a basis for further modifications as new components and kinetic parameters of the reactions are identified.

REFERENCE

1. Heinemann, C., et al., *Kinetics of the secretory response in bovine chromaffin cells following flash photolysis of caged Ca2+*. Biophysical Journal., 1994. **67**(6): p. 2546-57.
2.Berg, H.C.a.E.M.P.,, *Physics of chemoreception.* Biophys J, 1977. **20**(2): p. 193-219.
3.Gutman, M.a.E.N., *The dynamic aspects of proton transfer processes.* Biochim.Biophys Acta, 1990. **1015**: p. 391-414.
4.Oheim, M., et al., *Multiple stimulation-dependent processes regulate the size of the releasable pool of vesicles.* European Biophysics Journal., 1999. **28**(2): p. 91-101.
5.Plattner, H., A.R. Artalejo, and E. Neher, *Ultrastructural organization of bovine chromaffin cell cortex-analysis by cryofixation and morphometry of aspects pertinent to exocytosis.[erratum appears in J Cell Biol 1998 Feb 23;140(4):973].* Journal of Cell Biology., 1997. **139**(7): p. 1709-17.
6. Fasshauer, D. and M. Margittai, *A transient interaction of SNAP-25 and syntaxin nucleates SNARE assembly.* J Biol Chem, 2003.
7.Rickman, C., et al., *High Affinity Interaction of Sytaxin and SNAP-25 on The Plasma Membrane is Abolished by Botulinum Toxin E.* Journal of Biological Chemistry., 2003.
8.Lang, T., et al., *SNAREs are concentrated in cholesterol-dependent clusters that define docking and fusion sites for exocytosis.* EMBO Journal., 2001. **20**(9): p. 2202-13.
9.Margittai, M., et al., *Single-molecule fluorescence resonance energy transfer reveals a dynamic equilibrium between closed and open conformations of syntaxin 1.* Proc Natl Acad Sci U S A., 2003. **100**(26): p. 15516-15521.
10. Pabst, S., et al., *Selective interaction of complexin with the neuronal SNARE complex. Determination of the binding regions.* Journal of Biological Chemistry., 2000. **275**(26): p. 19808-18.
11. Ashery, U., et al., *Munc13-1 acts as a priming factor for large dense-core vesicles in bovine chromaffin cells.* EMBO Journal., 2000. **19**(14): p. 3586-96.
12. Moser, T. and E. Neher, *Estimation of mean exocytic vesicle capacitance in mouse adrenal chromaffin cells.* National Academy of Sciences of the United States of America, 1997. **94**: p. 6735-6740.
13. Voets, T., et al., *Intracellular calcium dependence of large dense-core vesicle exocytosis in the absence of synaptotagmin I.*PNAS., 2001. **98**(20): p. 11680-5.
14. Voets, T., *Dissection of three Ca^{2+}-dependent steps leading to secretion in chromaffin cells from mouse adrenal slices.* Neuron., 2000. **28**(2): p. 537-45.

ACNOWLEDGMENTS: The research in the Laser Laboratory for Fast Reactions in Biology is supported by the following research grants: The Israeli Science Foundation (472/01-2), the German-Israeli Foundation for Scientific Research and Development (G.I.F) (I –140-207.98) and the American Israeli Foundation Binational Science Foundation